SPACE CHARGE WAVES AS A DIAGNOSTIC TO MEASURE TRANSVERSE BEAM SIZE OF SPACE CHARGE DOMINATED BEAMS

Jayakar C.T. Thangaraj* D.W. Feldman, R.A. Kishek, S. Bernal, M. Reiser, D. Stratakis,
R.Feldman, D. Sutter, B. Beaudoin, C.Papadopoulos, I. Haber, P.G. O'Shea
Institute For Research in Electronics and Applied Physics
University of Maryland, College Park, MD 20742

Abstract

Intense charged particle beams are of great interest to many wide areas of application ranging from high-energy physics, light sources and energy recovery linacs, to medical applications. The University of Maryland Electron Ring (UMER) is a scaled model to investigate the physics of such intense beams. It uses a 10 keV electron beam along with other scaled beam parameters that model the larger machines but at a lower cost. Multi turn operation of the ring (3.6 m diameter) has been achieved for highly space charge dominated beams. Such, multi-turn operation requires a non-intercepting diagnostic for measuring the transverse beam size. Localized density or velocity variations on a space-charge dominated beam travel as space charge waves along the beam. The speed at which the space charge waves separate from each other depends on the beam current, energy and g-factor. In this work, we propose a diagnostic using deliberately-induced space charge waves to measure the beam size with multi-turn operation. We present and compare experimental results with self-consistent simulation.

INTRODUCTION

Intense beams are of significant interest in next generation linear colliders, FELs and ERLs [1, 2, 3]. Beam quality is crucial in all these applications. For example, too high an energy spreaad can create havoc to the operation of XFEL [4] . Hence, the beam has to be well diagnosed for successful operation of the machine. Fluctuations in intense beams, either as density or energy, propagate as space charge waves [5, 6]. Such space charge waves convert the density modulations in laboratory beams to energy modulations [7]. Energy modulations present in the beam gets converted back to density modulations when the beam goes through a dispersive section of an accelerator e.g. bunch compressor in LCLS [2]. Such oscillations between the energy space and density space disrupts the beam quality and hence the operation of the machine. Whenever there is a localized density or energy perturbation in an intense beam, space charge waves are launched [8]. Space charge waves are created in pairs and are classified as fast wave, when the wave travels toward the head of the beam and slow wave, when the wave travels toward the tail of the beam.

* jtobin@umd.edu, Department of Electrical and Computer Engineering, University of Maryland, College Park, USA

Previous work on space charge waves concentrated on generating such waves using various methods [9, 10, 11]. The waves separate at a speed called as the sound speed, which was found to be proportional to the beam current, on which the waves were launched. Neumann [12]demonstrated that introducing perturbation on intense beams can be very good terahertz radiation sources. In this work, we propose and demonstrate using space charge waves as a diagnostic tool [13] to measure the beam size of an intense beam. using a laser or using a induction cell,the beam can be perturbed in density or in energy thereby launching space charge waves. Once the waves start propagating, by measuring the propagating speed and the main beam current, the beam size can be estimated.

The University of Maryland Electron Ring (UMER) [14] uses a 10 keV electron beam with scaled parameters which model other bigger machines at much lower cost. Recently, multiturn operation was achieved. A technique was needed to measure the beam size without intercepting the beam. Space charge waves are a suitable diagnostics for measuring beams of intense space charge. As the speed of propagation of waves is proportional to the intensity of the beam,the more intense the beam is, the faster the waves propagate and hence easier to resolve the waves and measure the speed. The work is presented as follows: In section I, the theory of space charge waves is discussed following which the experimental setup is discussed in section II. The actual experiment and results is discussed in section III, which is followed by conclusion.

THEORY: ONE DIMENSIONAL COLD FLUID THEORY

The linear theory of space charge waves is based on a cold-fluid model [8]. In this model, a small initial perturbation is assumed and then both momentum and continuity equations are solved. The solution shows that the perturbations propagate along the beam in the form of waves. One of them has a phase velocity greater than the beam velocity called as a fast space-charge wave, while the other one has a phase velocity smaller than the beam velocity and hence called a slow space-charge wave.

The linear continuity and momentum equations can be represented as:

$$\frac{\partial \Lambda_1}{\partial t} + v_0 \frac{\partial v_1}{\partial z} + \Lambda_0 \frac{\partial \Lambda_1}{\partial t} = 0, \qquad (1)$$

Table 1: List of symbols and parameters used in 1-D cold fluid theory

Quantity	Symbol [1]
Line Charge Density $[C/m]$	Λ
Beam Current$[A]$	I
Beam velocity $[m/s]$	v
Geometry factor	g
Strength of velocity perturbation	δ
Strength of current perturbation	η

$$\frac{\partial v_1}{\partial t} + v_0 \frac{\partial v_1}{\partial z} \approx \frac{eE_z}{m\gamma^3} = \frac{-eg}{4\pi\varepsilon_0 m\gamma^5}\frac{\partial \Lambda_1}{\partial z} \tag{2}$$

where

$$\begin{aligned} \Lambda(z) &= \Lambda_0(z,t) + \Lambda_1(z,t) \\ v(z) &= v_0(z,t) + v_1(z,t) \\ I(z) &= I_0(z,t) + I_1(z,t) \end{aligned} \tag{3}$$

Now we apply the initial and boundary conditions. (a) There are no perturbation along the z-axis when $t < 0$. (b) At $z = 0$, and $t > 0+$, the localized current and velocity perturbation can be represented in the form

$$\begin{aligned} v_1(0,t) &= \delta v_0 h(t) \\ I_1(0,t) &= \eta I_0 h(t) \end{aligned} \tag{4}$$

Where δ is a small quantity corresponding to the strength of the velocity perturbation, η is a quantity whose values depend on the strength of the initial current perturbation. η can be either negative or positive depending on the operating conditions of the gun. $h(t)$ is a smooth function representing the shape of the perturbation and its amplitude is unity. From the above equations and $I = \Lambda v$, after neglecting the second order terms, the line charge density perturbation becomes,

$$\Lambda_1(0,t) = (\eta - \delta)\Lambda_0 h(t) \tag{5}$$

Now, by applying double Laplace transform for both t and z, the equation is reduced to solving algebraic equation in v_1, Λ_1 and I_1 in the $k - s$ domain from $z - t$ domain. After solving for the unknowns, an inverse Laplace transform is done to obtain the perturbed beam velocity, density and current in the time-space domain:

$$\begin{aligned} \Lambda_1(z,t) = &-\frac{\Lambda_0}{2}\left[\delta\frac{v_0}{c_s} - (\eta-\delta)\right] h\left(t - \frac{z}{v_0 - c_s}\right) \\ &+\frac{\Lambda_0}{2}\left[\delta\frac{v_0}{c_s} + (\eta-\delta)\right] h\left(t - \frac{z}{v_0 + c_s}\right) \end{aligned} \tag{6}$$

$$\begin{aligned} v_1(z,t) = &\frac{v_0}{2}\left[\delta - (\eta-\delta)\frac{c_s}{v_0}\right] h\left(t - \frac{z}{v_0 - c_s}\right) \\ &+\frac{v_0}{2}\left[\delta + (\eta-\delta)\frac{c_s}{v_0}\right] h\left(t - \frac{z}{v_0 + c_s}\right) \end{aligned} \tag{7}$$

$$\begin{aligned} I_1(z,t) = &-\frac{I_0}{2}\left[\delta\frac{v_0}{c_s} - \eta + (\eta-\delta)\frac{c_s}{v_0}\right] h\left(t - \frac{z}{v_0 - c_s}\right) \\ &+\frac{I_0}{2}\left[\delta\frac{v_0}{c_s} + \eta + (\eta-\delta)\frac{c_s}{v_0}\right] h\left(t - \frac{z}{v_0 + c_s}\right) \end{aligned} \tag{8}$$

As it can be seen from the solutions, the beam current contains two terms one: the slow wave term $h\left(t - \frac{z}{v_0 - c_s}\right)$, which moves towards the beam tail with a velocity c_s; the fast wave term $h\left(t - \frac{z}{v_0 + c_s}\right)$, which moves towards the head of the beam with sound speed c_s.

The "sound speed" $C_s = \sqrt{\frac{gg\Lambda_0}{4\pi\varepsilon_0 m\gamma^5}}$ is the velocity of the space charge waves in the beam frame, in analogy to the propagation of sound in gas, where $g = 2\ln\frac{b}{a}$; b is the beam pipe radius and a transverse beam radius. It should be noted that the space charge waves have the same shape as that of the initial perturbation but their amplitude and polarity are dependent on the strength of the initial perturbation and initial conditions.The same conclusion can also be arrived by constructing the dispersion relation for the space charge waves [8, 7]. The group velocity is equal to the phase velocity of the waves and hence they are dispersion free. In other words, the perturbation travels unaffected.

EXPERIMENTAL SETUP

A Minilite II Q-switched Nd: YAG laser from Continuum forms the source of optical power. The full-width half-maximum of the laser (FWHM) is around 5 ns.The pulse repetition frequency is set at 15Hz. By using the proper nonlinear crystals, light at either 355nm or 266nm can be produced. In these experiments, the third harmonic at 355nm was used. After the UV light is reflected by suitable dielectric mirrors, the light passes through a quartz window and is reflected by another mirror installed inside the chamber (IC1) and hits the cathode [15, 10]

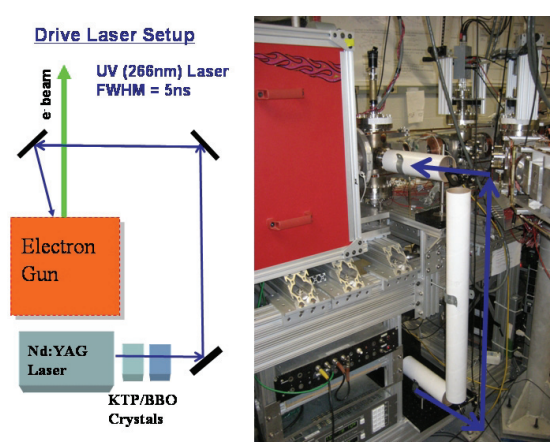

Figure 1: Schematic of the drive laser setup is shown on the left. The actual drive laser setup on UMER is shown on the right. The light path is shown with blue arrows.

DIAGNOSTICS

The induction cell [6] imposes an axial electric field in the beam direction by inducing a current through a parallel set of resistors straddling a glass section of the beam pipe. This glass section creates a discontinuity in the conduction path for the image current traveling along the beam pipe, such that the next path of least resistance is the housing that shields the termination end of the modulator. This path is essentially a short at low frequencies and yet contain an inductive component. So to increase the inductive term, as shown in the Figure,two high-frequency ferrite toroid are placed on either side of the glass gap region to choke off the high-voltage modulator and

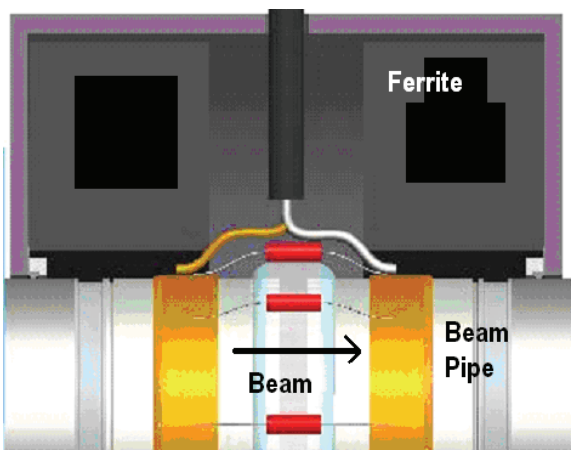

Figure 2: Induction Cell showing the ferrite toroid to choke the image current

allow an induced current to flow into the resistive path that straddles the glass gap region.

The modulator is composed of two BELKE high-voltage switches and circuitry to produce a positive and negative pulse with a full-width half-maximum (FWHM) of around 8nsec. The current modulator has a peak pulse voltage of 1kV with the capability of extending it too 3kV and a repetition rate that can be varied from 1Hz to 1MHz. As the beam propagates through the cell it can be pulsed at any point within the bunch, thus applying an axial electric field to accelerate and or decelerate any small segment of the bunch.

EXPERIMENT AND RESULTS

The beam is injected into the ring through injection optics and the beams goes around the ring for many turns. Every time it crosses the point of injection, a turn is counted. Beam loss has been observed for the first few turns. We believe it might be due to the injection optics. There are two current monitors to measure the total beam current. One is at z=3.83m (M1) and other one is at z=7.67m (M2) around the ring as shown in the Figure below. For the multi-turn beam, the signal from M1 and M2 is recorded in the scope without any density or energy modulation on the beam. Then a density modulation or energy modulation is introduced to the beam through the laser and the beam current signal from M1 and M2 is recorded with the perturbation. Care must be taken to ensure the perturbation is small compared to the main beam current. Typically values range from 5-10 percent of the main beam current. When the perturbation becomes too large, nonlinear effects starts to interfere with the measurment. In this ex-

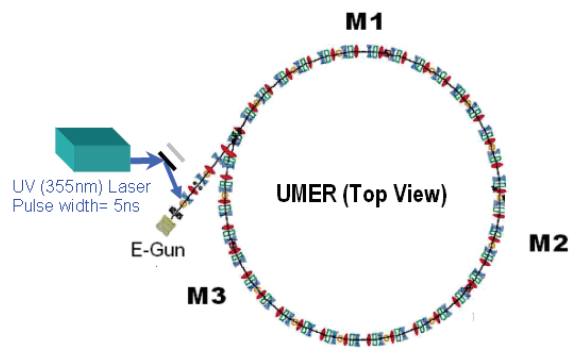

Figure 3: Top View of the University of Maryland Electron Ring (UMER)

periment, we assume there is no loss in the beam current within a given turn. In other words, the beam current does not change between M1 and M2. This is a very good assumption confirmed by measurement of signals from M1 and M2. sound speed from experimental data, let us assume that the waves travel a distance of δz in a time δt in the beam frame. The waves will separate at twice the sound speed from each other. So,the sound speed C_s will be equal to half of $\frac{\delta t \cdot v}{\delta z / v}$. Once we get the value of the sound speed, we calculate the g-factor from the formula $C_s = \sqrt{\frac{g g \Lambda_0}{4\pi\varepsilon_0 m \gamma^5}}$, the g-factor is related to the beamsize as $g = 2 \ln \frac{b}{a}$; b is the beam pipe radius and a transverse beam radius. . The measurement is repeated for various beam current and the value of the beamsize is recored for every turn.The variation of beam size for beam current with the turn number is shown in the graph below. Once the beam becomes emittance dominated, the waves move slowly and hence the beamsize cannot be calculated from the sound speed. A good guess, is the beam self-matches itself and hence the beam size remains constant thereafter.

CONCLUSION

An experimental technique to measure the transverse beam size of a space charge dominated beam is presented. Using a laser, space charge waves were launched on the beam and by measuring the speed at which the space charge waves separate the beam size was estimated over many turns. The experiment is conducted in UMER for various

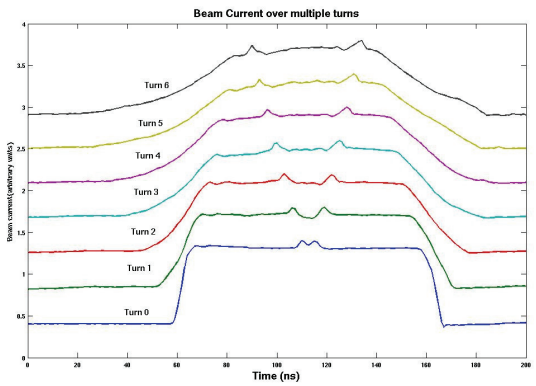

Figure 4: Space charge wave evolution over many turns. The spacecharge waves split into fast and slow waves

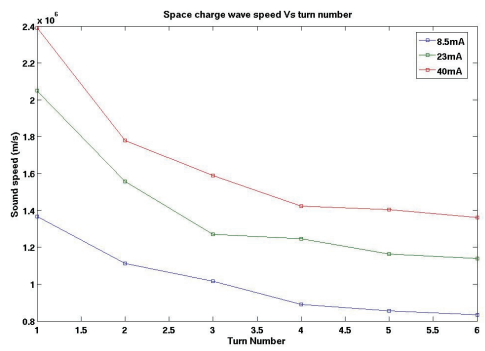

Figure 5: The speed of separation of the waves over multiple turns. As the beam current decreases, the speed of the waves decreases.

beam current and the shows good agreement with calculated values. By increasing the number of current monitors, the accuracy of this technique can be improved.The space charge waves technique can also be used to measure the g-factor in a FODO lattice for a long coasting beam.The space charge intensity [8] can be estimated using the space-charge wave technique after n turns. Estimating the emittance assuming a matched beam, we can calculate the space charge intensity at any turn.

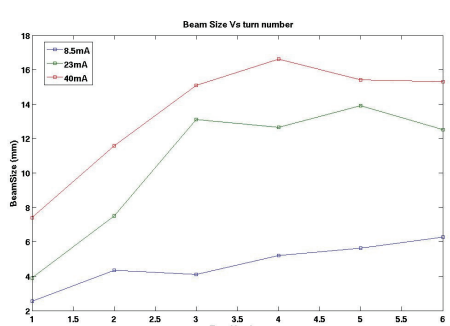

Figure 6: The transverse beam size Vs the number of turns. The beam seems to match itself to a specific value after few turns.

REFERENCES

[1] J. Brau et al., "International Linear Collider reference design report," ILC-REPORT-2007-001.

[2] J. Arthur et al., "Linac coherent light source (LCLS) conceptual design report," SLAC-R-593.

[3] M. Altarelli et al., "XFEL: The European X-Ray Free-Electron Laser. Technical design report," DESY-06-097.

[4] S. G. Biedron, Z. Huang, K.-J. Kim, S. V. Milton, G. Dattoli, A. Renieri, W. M. Fawley, H. P. Freund, H.-D. Nuhn, and P. L. Ottaviani, Phys. Rev. ST Accel. Beams **5**, 030701 (2002).

[5] J. Thangaraj et al., " Evolution of Laser Induced Perturbation and Experimental Observation of Space Charge Waves in the University of Maryland Electron Ring (UMER)," Proceeding of PAC,Albuquerque, NM, 2007.

[6] B. Beaudoin et al., "Application of induction module for energy perturbations in the University of Maryland Electron Ring," Proceeding of PAC,Albuquerque, NM, 2007.

[7] K. Tian et al., Phys. Rev. ST Accel. Beams **9**, 014201 (2006).

[8] M. Reiser, *Theory and design of charged particle beams* (WILEY-VCH Verlag GmBH & Co. KGaA,Weinheim, 2004).

[9] J. G. Wang, D. X. Wang, and M. Reiser, Phys. Rev. Lett. **71**, 1836 (1993).

[10] J. Harris, Ph.D. thesis, University of Maryland College Park (2005).

[11] H. Suk, J. Wang, and M. Reiser, Physics of Plasmas **3**, 669 (1996).

[12] J. Neumann et al., Nuclear Instruments and Methods in Physics Research A **507**, 498 (2003).

[13] J. G. Wang and M. Reiser, Review of Scientific Instruments **65**, 3444 (1994), `http://link.aip.org/link/?RSI/65/3444/1`.

[14] R. A. Kishek et al., "The University of Maryland Electron Ring (UMER) enters a new regime of high-tune-shift rings," Proceeding of 2007 PAC,Albuquerque, NM, 2007.

[15] Y. Huo, Master's thesis, University of Maryland College Park (2004).